polarization. In particular, we have considered the possibility that the entire $\Delta S=-\Delta Q$ amplitude is T violating (i.e., δ and ζ are purely imaginary) as proposed by Sachs.[22] If we require that the asymptotic transverse polarization be less than 2%, as suggested by present experiments,[23] then we find that the general features of the time dependence of the transverse polarization remain unchanged, although significant modifications occur. To detect these modifications, however, would require a greater experimental precision than is currently possible. Further details concerning this will be presented separately.

ACKNOWLEDGMENTS

I wish to thank Professor W. J. Willis for suggesting this investigation and for many useful conversations, Professor R. H. Socolow and Dr. L. H. Chan for guidance and encouragement during the course of this work, for many helpful suggestions, and for critical comments on the manuscript, Professor J. Sandweiss for discussions on the experimental aspects of the problem, and Professor R. K. Adair and Professor S. W. MacDowell for a reading of the manuscript.

[22] R. G. Sachs, Phys. Rev. Letters 13, 288 (1964).
[23] K. K. Young, M. J. Longo, and J. A. Helland, Phys. Rev. Letters 18, 806 (1967).

PHYSICAL REVIEW D VOLUME 3, NUMBER 1 1 JANUARY 1971

Double-Regge Analysis of Single-Pion Production in π^-p Interactions at 8 GeV/c*

W. D. Shephard, A. R. Dzierba,† N. N. Biswas, N. M. Cason, V. P. Kenney, and J. A. Poirier
Department of Physics, University of Notre Dame, Notre Dame, Indiana 46556
(Received 12 June 1970)

A double-Regge model (DRM) has been applied to $n\pi^+\pi^-$ and $p\pi^-\pi^0$ final states produced in π^-p interactions at 8 GeV/c incident beam momentum. Application of the model has been limited to the energy region where all two-body final-state masses are large. Some difficulty exists in trying to understand the qualitative features of all the data in terms of the model. Parameters of the model have been determined for those events which display features consistent with the DRM. These parameters are used to predict distributions in various kinematic variables.

I. INTRODUCTION

There has been much interest recently in describing strong interactions involving three or more final-state particles in terms of various multiparticle-exchange mechanisms. There have been several detailed formulations of these models. Among these are the un-Reggeized double-particle-exchange model of Joseph and Pilkuhn[1] and the double-Regge-pole-exchange models (DRM) of Chan *et al.*,[2] Bali *et al.*,[3] and Zachariasen and Zweig.[4] Experimental consistency with the DRM has been reported in describing $\pi\pi N$ and KKN final states[2] as well as other quasi-three-body final states.[5–8] Reggeized multiperipheral models have also been used to give qualitative agreement with experiment for higher-multiplicity final states.[9] The attractive feature of the DRM is that one can use information from two-body processes to describe interactions with three bodies in the final state.

We have employed the DRM to study the reactions

$$\pi^-p\to n\pi^+\pi^- \quad (1)$$

and

$$\pi^-p\to p\pi^-\pi^0 \quad (2)$$

at 8 GeV/c. The formulation of the DRM and the form used for the amplitude are discussed in Sec. II. In Sec.

* Work supported in part by the National Science Foundation.
† Present address: Lauritsen Laboratory of High Energy Physics, California Institute of Technology, Pasadena, Calif. 91109.
[1] J. Joseph and H. Pilkuhn, Nuovo Cimento 33, 1407 (1964).
[2] (a) Chan Hong-Mo, K. Kajantie, and G. Ranft, Nuovo Cimento 49A, 157 (1967); (b) Chan Hong-Mo, K. Kajantie, G. Ranft, W. Beusch, and E. Flaminio, *ibid.* 51A, 696 (1967).
[3] M. F. Bali, G. F. Chew, and A. Pignotti, Phys. Rev. 162, 1572 (1967); Phys. Rev. Letters 19, 614 (1967).
[4] F. Zachariasen and G. Zweig, Phys. Rev. 160, 1322 (1967); 160, 1326 (1967).
[5] R. Lipes, G. Zweig, and W. Robertson, Phys. Rev. Letters 22, 433 (1969); see also G. Zweig, ANL Report No. ANL/HEP 6909, 1968 (unpublished).
[6] For a brief survey of double peripheral models with references up to January 1968, see S. Ratti, in *Proceedings of the Topical Conference on High-Energy Collisions of Hadrons, CERN, 1968* (Scientific Information Service, Geneva, 1968), p. 611; see also reports by O. Czyzewski and Chan Hong-Mo, in *Proceedings of the Fourteenth International Conference on High-Energy Physics, Vienna, 1968*, edited by J. Prentki and J. Steinberger (CERN, Geneva, 1968).
[7] J. D. Jackson, Rev. Mod. Phys. 42, 12 (1970).
[8] E. L. Berger, Phys. Rev. Letters 21, 701 (1968); Phys. Rev. 179, 1567 (1969).
[9] Chan Hong-Mo, J. Loskiewicz, and W. W. M. Allison, Nuovo Cimento 57A, 93 (1968).

III the qualitative features of the data are discussed in terms of the DRM. The fitting procedure and the quantitative results obtained are presented in Sec. IV. Section V includes a discussion of the successes and difficulties encountered with the model in fitting our experimental data.

II. DOUBLE-REGGE-EXCHANGE MODEL

The DRM seeks to describe reactions of the type

$$1+2 \rightarrow 3+4+5 \tag{3}$$

using the graph of Fig. 1 (hereafter referred to as the DRM graph), where a and b are exchanged trajectories. The five kinematical invariants necessary for a complete description of a reaction of type (3) have been chosen (refer to Fig. 1) as $s \equiv s_{12}$, s_{34}, s_{45}, t_{13}, and t_{25}, where

$$s_{jk}=(p_j+p_k)^2\,,$$

and (4)

$$t_{ij}=(p_i-p_j)^2\,,$$

with

$$p_k=(\mathbf{p}_k,E_k) \quad \text{and} \quad E_k=(\mathbf{p}_k{}^2+m_k{}^2)^{1/2}.$$

The s_{jk} are squares of two-body effective masses and the t_{ij} are the momentum-transfer variables. The total center-of-mass (c.m.) energy squared is given by s. These variables will be used to define the region of application of the model and the form of the amplitude assumed for reaction (3). In our application of the model, s is held fixed.

A. Region of Application

The kinematic region in which the DRM is expected to be applicable is illustrated on the Dalitz plot of s_{45} vs s_{34} sketched in Fig. 2. Within the kinematically allowed region for events of type (3), regions A, B, and C correspond to events with low s_{34}, s_{45}, and s_{35}, respectively. In the reactions for which the DRM is used these regions are usually dominated by quasi-two-body final states involving resonance production. Although the concept of duality[10] suggests that a form of the DRM might provide valid results averaged over the resonances, we have not attempted to apply the model in these regions. In region D, characterized by relatively high effective masses for all two-body combinations, resonance production is expected to be slight at the energy of current experiments. Thus we restrict the application of the model to region D where all two-body effective masses are large compared to the masses of copiously produced resonances.

The restriction to region D is also desirable for another reason. For two-body processes the amplitude can be approximated by the exchange of a Regge pole in the t channel at high c.m. energies. Correspondingly, the DRM should describe the high-energy region in s_{45} (s_{34}) in terms of the exchange of $b(a)$ in the t channel. Therefore, the model should be applicable in the center of the Dalitz plot where s_{34} and s_{45} in addition to s are large.

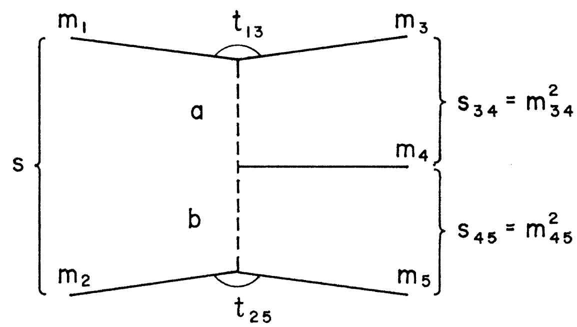

FIG. 1. DRM graph describing the processes under discussion in this paper. The dashed lines a and b represent the exchanged trajectories. The square of the total c.m. energy of incident particles m_1 and m_2 is s. The squares of the final-state two-body effective masses m_{jk} are denoted by s_{jk}. The square of the four-momentum transfer between the incident particle m_i and final particle m_j is t_{ij}.

B. DRM Amplitude

The generalization from two- to three-body processes suggests the following form of the amplitude for the

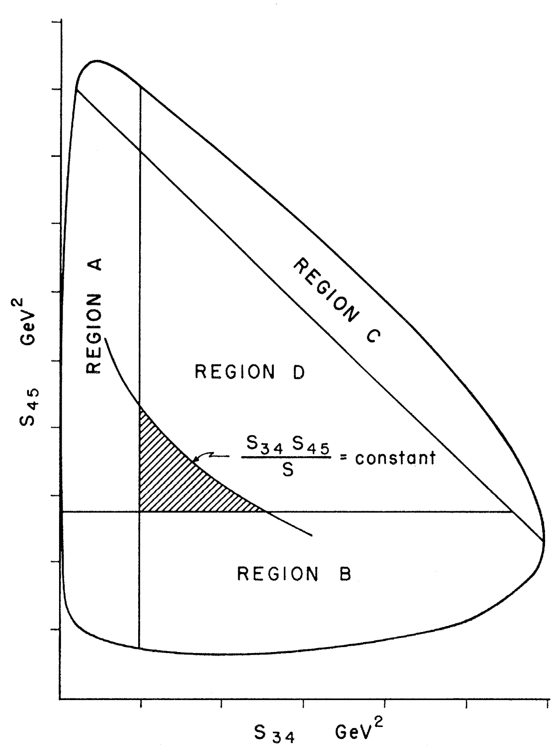

FIG. 2. Sketch of the Dalitz plot for the process $1+2 \rightarrow 3+4+5$. Regions A, B, and C correspond to portions of the Dalitz plot where one or more two-body effective masses are small and where resonance production is expected to be important. Region D is the region in which we apply the DRM. The region of "cornering" for the DRM graph of Fig. 1 is shaded.

[10] R. Dolen, D. Horn, and C. Schmid, Phys. Rev. **166**, 1768 (1968); G. F. Chew and A. Pignotti, Phys. Rev. Letters **20**, 1078 (1968).

DRM graph[2]:

$$\mathrm{Amp}(s_{34},s_{45},t_{13},t_{25})=\gamma_a(t_{13})\gamma_b(t_{25})\xi_a\xi_b\gamma(t_{13},t_{25},\omega)\times\left(\frac{s_{34}}{s_0}\right)^{\alpha_a(t_{13})}\left(\frac{s_{45}}{s_0}\right)^{\alpha_b(t_{25})}. \quad (5)$$

As in two-body Regge processes, we have $\gamma_a(t_{13})$ and $\gamma_b(t_{25})$ describing the three-particle coupling at the vertices ($1a3$) and ($2b5$), respectively. The $\xi_a(t_{13})$ and $\xi_b(t_{25})$ are the signature factors given by

$$\xi(t)=\frac{1\pm e^{-i\pi\alpha(t)}}{\Gamma[1+\alpha(t)]\sin[\pi\alpha(t)]}. \quad (6)$$

The energy dependence of the amplitude is given by $(s_{45}/s_0)^{\alpha_b(t_{25})}$ and $(s_{34}/s_0)^{\alpha_a(t_{13})}$, where $\alpha(t)$ is the Regge trajectory function and s_0 is a scale factor (we have used $s_0=1$ GeV^2). All the above factors can in principle be determined from experimental information for two-body processes. The factor $\gamma(t_{13},t_{25},\omega)$ is peculiar to the case where there are three particles in the final state. It describes the coupling of the two exchanged trajectories to the middle particle (particle 4 of Fig. 1). It has been shown by several authors[2,3,11] using the theory of complex angular momentum that this function depends only on t_{13}, t_{25}, and ω, where

$$\cos\omega=\frac{(\mathbf{p}_1\times\mathbf{p}_3)\cdot(\mathbf{p}_2\times\mathbf{p}_5)}{|\mathbf{p}_1\times\mathbf{p}_3|\,|\mathbf{p}_2\times\mathbf{p}_5|} \quad (7)$$

in the coordinate system where $\mathbf{p}_4=0$. The distribution of this angle, often referred to as the Toller angle, is a measure of the relative polarization of the trajectories a and b. When the amplitude is squared and signature factors are absorbed,[12] the result is

$$|\mathrm{Amp}|^2=\beta_a(t_{13})\beta_b(t_{25})\beta(t_{13},t_{25},\omega)\times\left(\frac{s_{34}}{s_0}\right)^{2\alpha_a(t_{13})}\left(\frac{s_{45}}{s_0}\right)^{2\alpha_b(t_{25})}. \quad (8)$$

The explicit functional dependence of $\beta_a(t_{13})$ and $\beta_b(t_{25})$ on t_{13} and t_{25} is not given by Regge theory. However, it is known from two-body processes that the dependence of β_a and β_b on t is approximately exponential. The assumption is made that $\beta(t_{13},t_{25},\omega)$ is also exponentially dependent on t_{13} and t_{25}. The functional dependence of $\beta(t_{13},t_{25},\omega)$ on ω is unknown *a priori*. We assume that $\beta(t_{13},t_{25},\omega)$ is independent of ω. The validity of this assumption has been checked experimentally.[13] The trajectory functions are assumed to be linear in t, i.e.,

$$\alpha(t)=\alpha(0)+\alpha'(0)t. \quad (9)$$

With the above assumptions about the dependence of the trajectories and residue functions on t_{13}, t_{25}, and ω, we have

$$|\mathrm{Amp}|^2=\mathrm{const}\times e^{2At_{13}}e^{2Bt_{25}}\left(\frac{s_{34}}{s_0}\right)^{2\alpha_a(0)}\left(\frac{s_{45}}{s_0}\right)^{2\alpha_b(0)}, \quad (10)$$

where

$$A=D_a+\alpha_a'(0)\ln(s_{34}/s_0)$$

and

$$B=D_b+\alpha_b'(0)\ln(s_{45}/s_0).$$

The Regge parameters (the slopes and intercepts for trajectories a and b) can be estimated from two-body processes. The diffractive parameters D_a and D_b must be determined for three-body final states since they cannot be determined from two-body scattering. We are thus left with an amplitude for reaction (3) in terms of the four independent invariants, the four known Regge parameters, and two diffractive parameters to be determined from the data.

C. Qualitative DRM Predictions

As mentioned earlier the DRM describes high-energy reactions which are dominated by poles in the momentum-transfer variables. Thus we expect the distributions in t_{13} and t_{25} to peak at low values. This characteristic of the DRM leads to other qualitative predictions about the events it can describe: (1) "cornering" in the Dalitz plot and (2) "ordering" of the longitudinal components of c.m. momenta.

Consider the distribution of DRM events in the central region of the Dalitz plot. The expected simultaneous dominance of small t_{13} and t_{25} implies that the effective mass of particles 3 and 5 will tend to be near its maximum allowed value. The events described by Fig. 1 will occupy the shaded corner of the Dalitz plot of Fig. 2 where s_{35} is large. Chan *et al.*[2] have given a more quantitative description of this cornering effect. If the angle ω is expressed in terms of the kinematical invariants and the vertices are assumed to be diffractive, the condition $\cos\omega\geq -1$ implies

$$[(-t_{13})^{1/2}+(-t_{25})^{1/2}]^2+m_4^2\geq s_{34}s_{45}/s, \quad (11)$$

and for small $|t_{13}|$ and $|t_{25}|$, $(s_{34}s_{45})/s\leq m_4^2$. The equation $(s_{34}s_{45})/s=m_4^2$ defines a hyperbola (see Fig. 2) limiting the events to one corner of region D in the Dalitz plot. The strength of this cornering is determined by the mass of the middle particle 4. When m_4 is large, cornering is less pronounced. Chan *et al.*[2] have also noted that, for a fixed $(s_{34}s_{45})/s$, a large m_4 allows smaller values of $|t_{13}|$ and $|t_{25}|$. Thus graphs with large m_4 may be significant even if they involve suppressed exchanges.

For a reaction such as (1) or (2) there are six possible ways of ordering the three final-state particles to

[11] M. S. K. Razmi, Nuovo Cimento **31**, 615 (1964).

[12] In our use of the DRM, we have not explicitly included the t dependence of the signature factors but have treated them as constants, as was done in the theoretical formulations of the model developed in Refs. 2 and 5.

[13] In Sec. IV we show that the distribution calculated for ω using this assumption is consistent with our data. The same assumption has been found valid in other reactions (see Ref. 8).

correspond with Fig. 1. These may be considered as three pairs where members of a pair have the same middle particle 4. Events described by a given pair occupy a distinct corner of the Dalitz plot. The center of the Dalitz plot is thus expected to be depopulated. Some of the six orderings may require exchanges which are expected to be suppressed. If both orderings of a pair are thus suppressed, the density of events in the corresponding corner of the Dalitz plot is expected to be small.[14]

The dominance of small $|t_{13}|$ and $|t_{25}|$ inherent in the model also provides a method for assigning individual events of a reaction to one of the six possible DRM orderings. If the c.m. momenta of final-state particles are decomposed into longitudinal and transverse components p_l and p_t with respect to the direction of particle 1, the longitudinal components for particles 3 and 5 are expected to be near the maximum allowed values and to be positive and negative, respectively. Particle 4 should have a small longitudinal component and whatever transverse component is required to satisfy momentum conservation. If we define $\tan\theta = p_t/p_l$, the distribution of this angle for particle 4 will peak near 90° unless the average p_t is very small.

The model suggests that individual events be assigned to specific orderings on the basis of final-state longitudinal momenta such that $p_l(3)>p_l(4)>p_l(5)$. Although such assignments preclude the possibility of studying the tails of momentum-transfer distributions, they should give qualitatively reasonable results. Another possible criterion is the assignment of each event so that $|t_{13}+t_{25}|$ is minimized. In practice, we have found that these criteria lead to essentially the same assignments.

Van Hove[15] has suggested a convenient way in which to display the relationships between the longitudinal momenta, especially for three-body final states. Events are represented as points on a "longitudinal phase-space plot." A three-body final state is represented in terms of polar coordinates q and Ω, where

$$\begin{aligned} q&=[p_l^2(3)+p_l^2(4)+p_l^2(5)]^{1/2}\,,\\ \sin\Omega&=(\sqrt{\tfrac{3}{2}})p_l(3)/q\,,\\ \cos\Omega&=[p_l(5)-p_l(4)]/\sqrt{2}q\,. \end{aligned} \tag{12}$$

If the events are peripheral in nature as evidenced by small transverse momenta the points will tend to cluster near the boundary of the allowed region of the plot. Events corresponding to a given one of the six possible orderings of the final-state longitudinal momenta occupy a definite 60° range in Ω. Thus it is easy to see the classification of events by longitudinal momentum ordering on a plot of Ω.

[14] In the reactions under consideration this unique situation occurs in the case of the $n\pi^+\pi^-$ final state where both orderings in the pair with the π^- as the middle particle require exchanges which we expect to be suppressed.

[15] L. Van Hove, Nucl. Phys. **B9**, 331 (1969).

III. QUALITATIVE APPLICATION OF DRM AT 8 GeV/c

The data to be examined in terms of the DRM were obtained from two separate exposures in the BNL 80-in. hydrogen bubble chamber at π^- beam momenta of 8.05 and 7.9 GeV/c analyzed at the University of Notre Dame and the University of Pennsylvania, respectively. A total of 2448 events were identified as reaction (1) and 1147 events as reaction (2) on the basis of kinematic fits and consistent ionization. Experimental details are presented elsewhere.[16]

A limited sample of the data was selected for analysis in terms of the DRM. The central region of the Dalitz plot was defined by requiring $s_{\pi\pi}>2$ GeV^2 and $s_{\pi N}>3$ GeV^2. These cuts were chosen to exclude most resonant structure in the various two-body effective masses. They represent a compromise designed to include a statistically significant data sample while limiting analysis, so far as possible, to the range of two-body masses where the DRM amplitude should be applicable. The above cuts leave 12% (303 events) of reaction (1) and 10% (118 events) of reaction (2) in the sample.

After these cuts were made, events corresponding to the six possible DRM channels were selected on the basis of ordering of the longitudinal momenta. The notation (a,b,c) will be used to designate the ordering for those events for which $p_l(a)>p_l(b)>p_l(c)$. Figures 3 and 4 show the various DRM graphs for reactions (1) and (2), together with the possible exchanges allowed and the numbers of events from the center of the Dalitz plot assigned to each ordering. (Note that in some of the graphs exchange of bosons with $I=2$ and/or of baryons would be required.)

The Dalitz plots for reactions (1) and (2) are shown in Figs. 5 and 6. The region of application of the model, defined by $s_{\pi\pi}>2$ GeV^2 and $s_{\pi N}>3$ GeV^2, is enclosed by solid lines. The depletion in the center of this region predicted by the DRM is indeed evident.

In Figs. 7 and 8 are shown the Van Hove longitudinal phase-space scatter plots for events of reactions (1) and (2), respectively. Plots are shown for all events and for the events in the central region of the Dalitz plot. As expected for peripheral events, the points are predominantly near the boundaries of the plots. As seen in Figs. 7(b) and 8(b), this characteristic is found for events in the center of the Dalitz plot as well as for all events. In Figs. 9 and 10 are shown the Ω distributions for all events of reactions (1) and (2) and for the events in the center of the Dalitz plot. In Figs. 9(b) and 10(b) can be seen peaks in the Ω distribution corresponding to particular orderings of the longitudinal momenta listed in Figs. 3 and 4. The angle Ω has been defined for re-

[16] J. A. Poirier, N. N. Biswas, N. M. Cason, I. Derado, V. P. Kenney, W. D. Shephard, and E. H. Synn, and H. Yuta, W. Selove, R. Ehrlich, and A. L. Baker, Phys. Rev. **163**, 1462 (1967); S. J. Barish, W. Selove, N. N. Biswas, N. M. Cason, P. B. Johnson, V. P. Kenney, J. A. Poirier, W. D. Shephard, and H. Yuta, *ibid.* **184**, 1385 (1969).

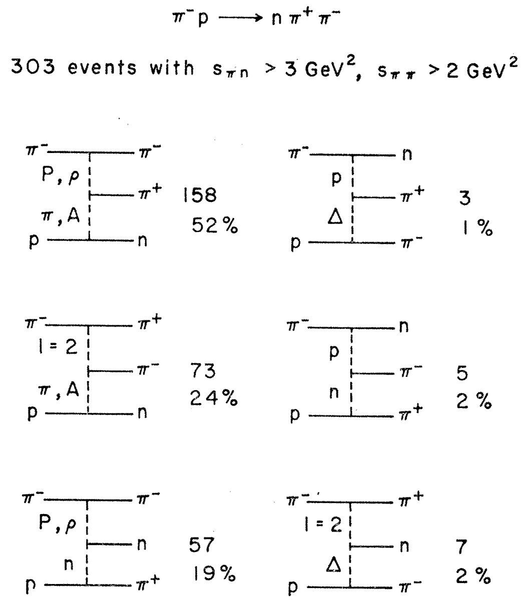

FIG. 3. DRM graphs for the reaction $\pi^- p \to n\pi^+\pi^-$. The numbers and percentages of events which are assigned to the various graphs on the basis of longitudinal momentum ordering are listed. Only events with $s_{\pi n}>3$ GeV^2 and $s_{\pi\pi}>2$ GeV^2 have been considered.

actions (1) and (2) so that particle (3) is the π^-, particle (4) the π^+ or π^0, and particle (5) the n or p. In Table I are listed the possible orderings for reactions (1) and (2) and the ranges of Ω to which they correspond.

The different orderings of the final-state particles are discussed in the remainder of this section.

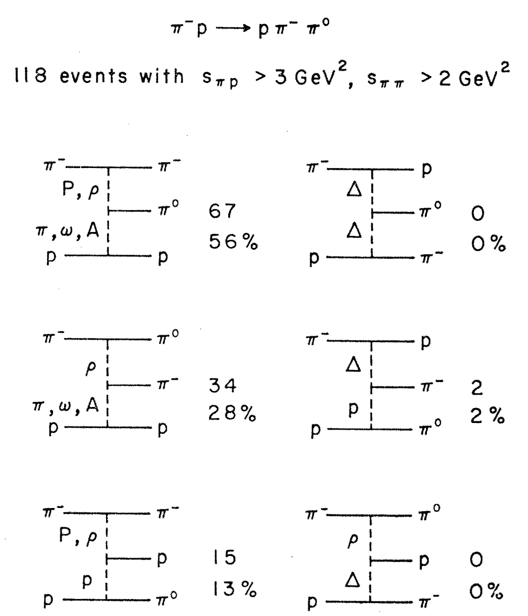

FIG. 4. DRM graphs for the reaction $\pi^- p \to p\pi^-\pi^0$. The numbers and percentages of events which are assigned to the various graphs on the basis of longitudinal momentum ordering are listed. Only events with $s_{\pi p}>3$ GeV^2 and $s_{\pi\pi}>2$ GeV^2 have been considered.

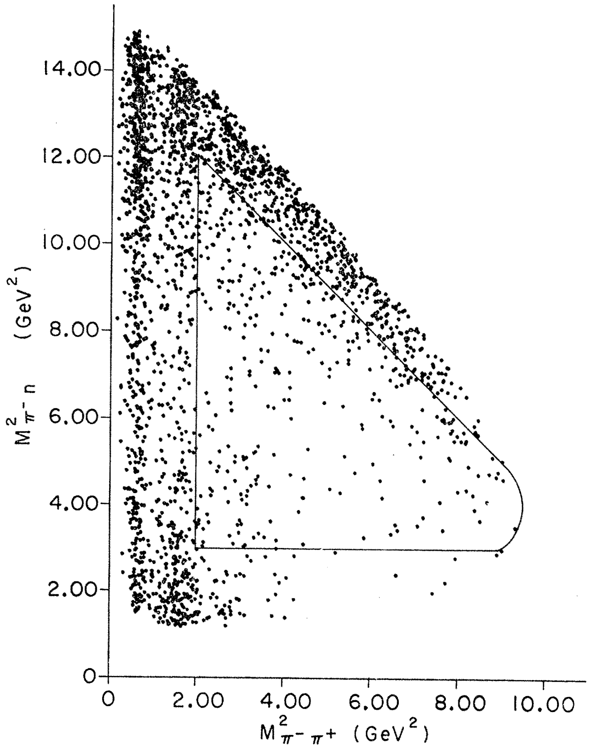

FIG. 5. Dalitz plot for the reaction $\pi^- p \to n\pi^+\pi^-$ at 8 GeV/c. The region with $s_{\pi\pi}>2$ GeV^2, $s_{\pi n}>3$ GeV^2 in which we have applied the DRM is outlined.

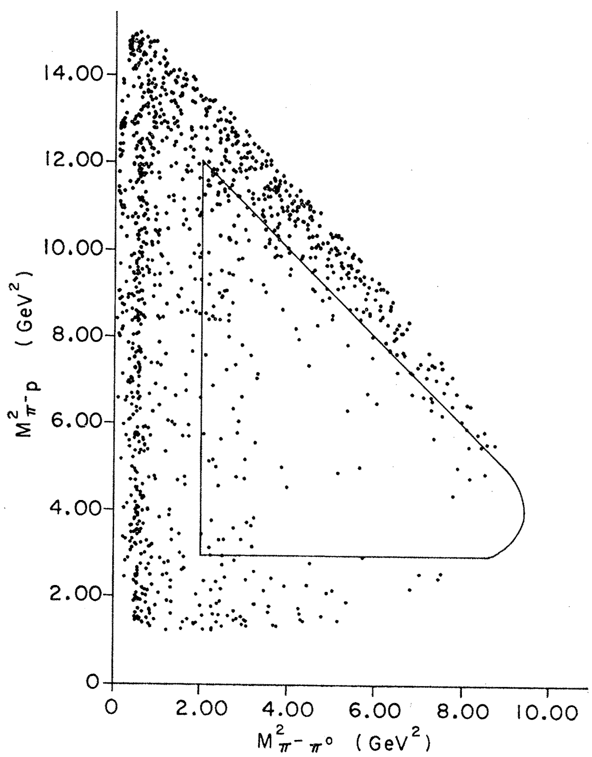

FIG. 6. Dalitz plot for the reaction $\pi^- p \to p\pi^-\pi^0$ at 8 GeV/c. The region with $s_{\pi\pi}>2$ GeV^2, $s_{\pi p}>3$ GeV^2 in which we have applied the DRM is outlined.

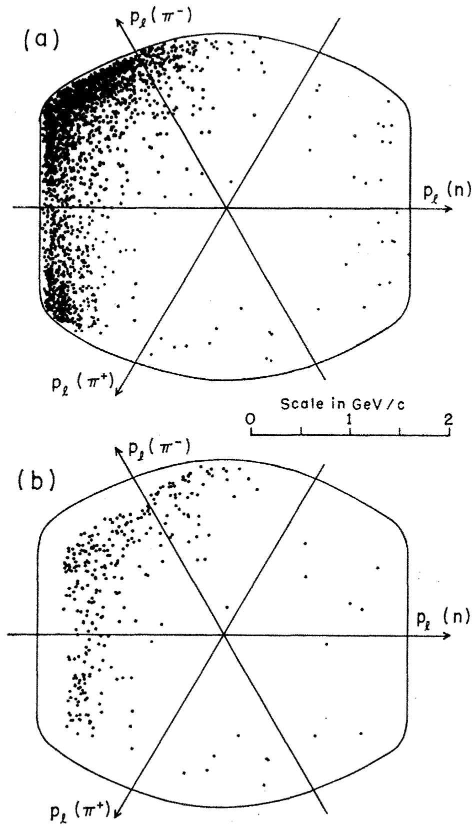

FIG. 7. Longitudinal phase-space plots for events of the reaction $\pi^-p\rightarrow n\pi^+\pi^-$: (a) Plot for all events and (b) plot for events with $s_{\pi\pi}>2$ GeV^2 and $s_{\pi n}>3$ GeV^2.

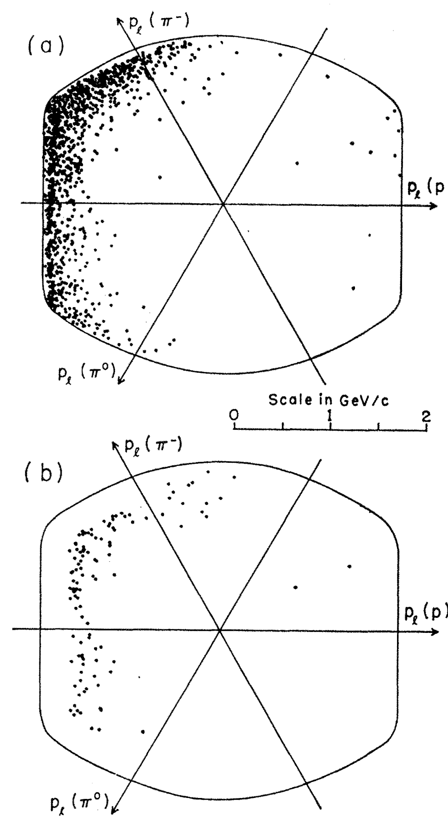

FIG. 8. Longitudinal phase-space plots for events of the reaction $\pi^-p\rightarrow p\pi^-\pi^0$: (a) Plot for all events and (b) plot for $s_{\pi\pi}>2$ GeV^2 and $s_{\pi p}>3$GeV^2.

A. (π^-,π^+,n) and (π^-,π^0,p) Orderings

Orderings such as (π^-,π^+,n) and (π^-,π^0,p), where no charge-2 or baryon exchanges are required, are expected to be most important. This is experimentally confirmed (see Figs. 3 and 4) since over 50% of the events in the center of the Dalitz plot correspond to these orderings. The Dalitz plots for these subsets of events are shown in Fig. 11. Strong cornering is seen corresponding to a dominance of large $\pi^-n(\pi^-p)$ masses as predicted by the DRM for the case where the $\pi^+(\pi^0)$ is the middle particle.

It may be shown that the cornering is not simply a consequence of the way the events have been ordered on the basis of longitudinal momenta. In Fig. 12 is shown a Dalitz plot for a sample of $\pi_1\pi_2N$ events generated by Monte Carlo methods according to phase space to which the same criteria have been applied so that $p(\pi_1)$

TABLE I. Correspondence between longitudinal momentum ordering and Van Hove angle Ω.

Ordering	Range of Ω
(π^-,π^+,n), (π^-,π^0,p)	$90°\leq\Omega\leq150°$
(π^+,π^-,n), (π^0,π^-,p)	$150°\leq\Omega\leq210°$
(π^+,n,π^-), (π^0,p,π^-)	$210°\leq\Omega\leq270°$
(n,π^+,π^-), (p,π^0,π^-)	$270°\leq\Omega\leq330°$
(n,π^-,π^+), (p,π^-,π^0)	$330°\leq\Omega\leq30°$
(π^-,n,π^+), (π^-,p,π^0)	$30°\leq\Omega\leq90°$

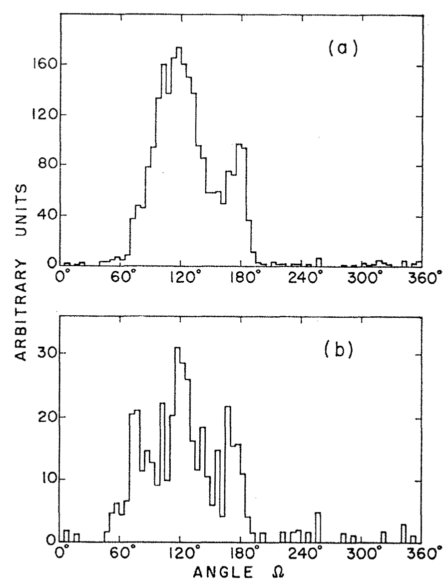

FIG. 9. Distributions of the Van Hove angle Ω for events of the reaction $\pi^-p\rightarrow n\pi^+\pi^-$: (a) Distribution for all events and (b) distribution for events with $s_{\pi\pi}>2$ GeV^2 and $s_{\pi n}>3$ GeV^2.

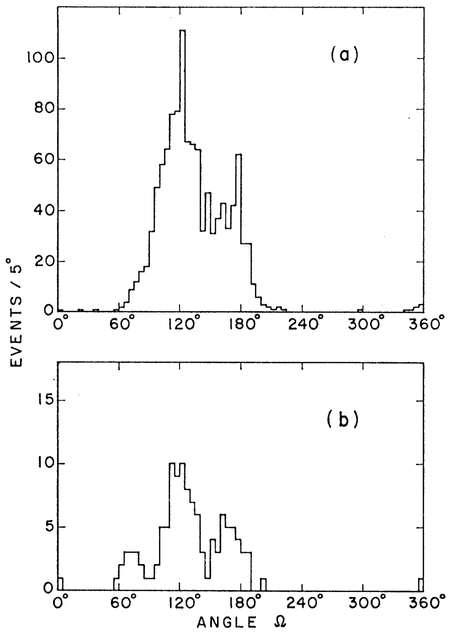

FIG. 10. Distribution of the Van Hove angle Ω for events of the reaction $\pi^- p \rightarrow p\pi^-\pi^0$: (a) Distribution for all events and (b) distribution for events with $s_{\pi\pi} > 2$ GeV² and $s_{\pi p} > 3$ GeV².

$> p(\pi_2) > p(N)$. Very little cornering is observed. Thus the cornering is due to the double peripheral nature of the data.

The momentum transfer distributions for the real events are shown in Fig. 13. All of these distributions are peaked at small $|t|$ and are roughly exponential in form as predicted for the DRM. The t distributions at the nucleon vertex are more sharply peaked than the t distributions at the meson vertex.

These events are the simplest of our data to understand and interpret in terms of the DRM. Comparisons with quantitative calculations have been made. The results will be presented in Sec. IV.

B. (n,π^+,π^-) and (p,π^0,π^-) Orderings

Events assigned to the (n,π^+,π^-) and (p,π^0,π^-) orderings would tend to occupy the same corner of the

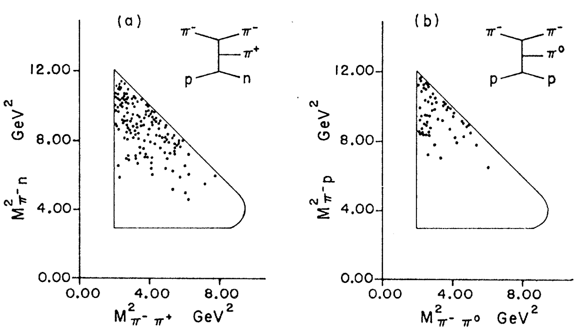

FIG. 11. Dalitz plots for events of the orderings (a) (π^-,π^+,n) and (b) (π^-,π^0,p) at 8 GeV/c.

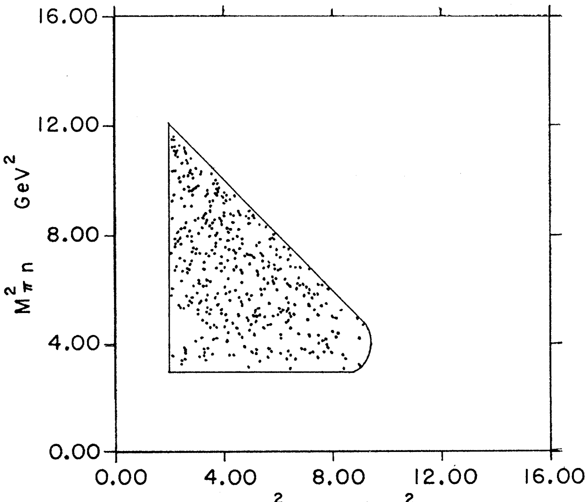

FIG. 12. Dalitz plot for Monte Carlo events of the type $\pi N \rightarrow \pi_1\pi_2 N$ which have been generated according to pure phase space and selected so $s_{\pi\pi} > 2$ GeV², $s_{\pi N} > 3$ GeV², and $p_t(\pi_1) > p_t(\pi_2) > p_t(N)$.

Dalitz plot as the dominant (π^-,π^+,n) and (π^-,π^0,p) events. However, their description in terms of the DRM would require both exchange trajectories to be baryon trajectories. In the (p,π^0,π^-) case both exchanges must

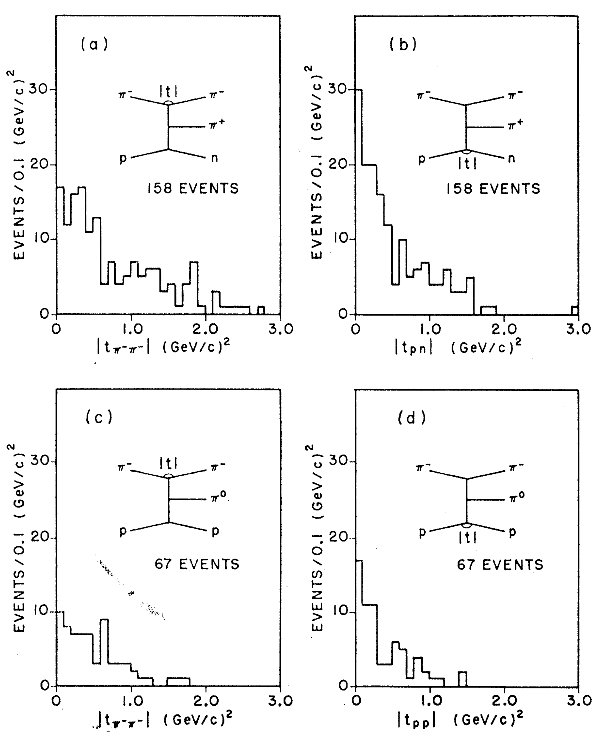

FIG. 13. Momentum transfer distributions for events of the orderings (π^-,π^+,n) and (π^-,π^0,p) at 8 GeV/c: (a) distribution of $t_{\pi^-\pi^-}$ for (π^-,π^+,n) events; (b) distribution of t_{pn} for (π^-,π^+,n) events; (c) distribution of $t_{\pi^-\pi^-}$ for (π^-,π^0,p) events; and (d) distribution of t_{pp} for (π^-,π^0,p) events.

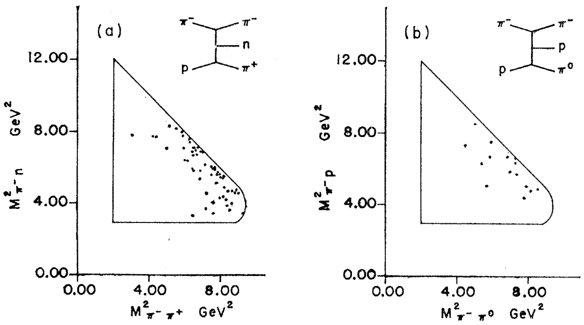

FIG. 14. Dalitz plots for events of the orderings (a) (π^-,n,π^+) and (b) (π^-,p,π^0) at 8 GeV/c.

be $I=\frac{3}{2}$ baryons, while in the (n,π^+,π^-) case one exchange must be $I=\frac{3}{2}$ while the other may be $I=\frac{1}{2}$. Since in two-body interactions baryon exchange is observed to be considerably suppressed with respect to meson exchange, these channels should be greatly suppressed if the DRM is valid. This suppression is observed (see Figs. 3 and 4).

C. (π^-,n,π^+) and (π^-,p,π^0) Orderings

Events corresponding to the (π^-,n,π^+) and (π^-,p,π^0) orderings would occupy the corner of the Dalitz plot with large $s_{\pi\pi}$. As shown in Figs. 3 and 4, 19% of the reaction (1) events and 13% (15) of the reaction (2) events in the center of the Dalitz plot have been assigned to these channels. In terms of the DRM they involve one baryon ($I=\frac{1}{2}$ or $\frac{3}{2}$) and one meson ($I=0$, 1, or 2) exchange and have a nucleon as the middle particle.

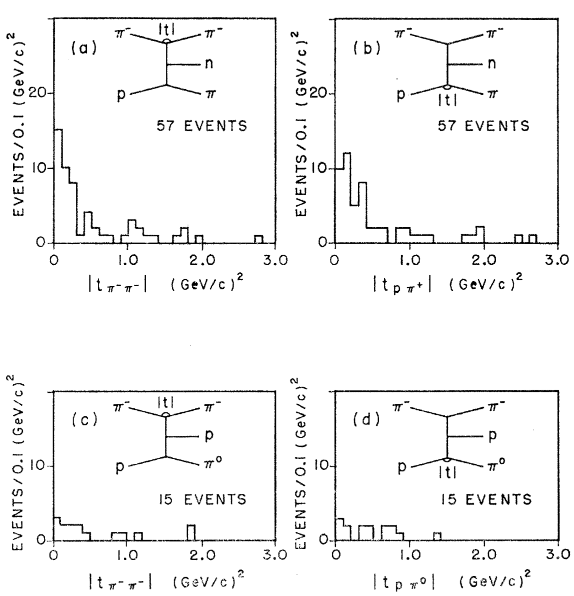

FIG. 15. Momentum transfer distributions for events of the orderings (π^-,n,π^+) and (π^-,p,π^0) at 8 GeV/c: (a) distribution of $t_{\pi^-\pi^-}$ for (π^-,n,π^+) events; (b) distribution of $t_{p\pi^+}$ for (π^-,n,π^+) events; (c) distribution of $t_{\pi^-\pi^-}$ for (π^-,p,π^0) events; and (d) distribution of $t_{p\pi^0}$ for (π^-,p,π^0) events.

The large mass of the middle particle implies a decrease in the strength of cornering on the Dalitz plot for these channels, as observed in Fig. 14. It also implies a kinematical enhancement for these channels[2] which might counteract the suppression expected due to baryon exchange so they can compete with channels involving only meson exchange. The momentum transfer distributions for these events are shown in Fig. 15.

D. (π^+,n,π^-) and (π^0,p,π^-) Orderings

Both of the orderings (π^+,n,π^-) and (π^0,p,π^-), which would occupy the same corner of the Dalitz plot as the events discussed in Sec. III C, would also require one baryon and one meson exchange. However, the baryon must have $I=\frac{3}{2}$ in these cases. Since the lowest $I=\frac{3}{2}$ baryon trajectory lies above the lowest $I=\frac{1}{2}$ trajectory, contributions due to $I=\frac{3}{2}$ exchange are expected to be suppressed relative to $I=\frac{1}{2}$ exchange. This suppression is consistent with experiment as shown in Figs. 3 and 4.

E. (n,π^-,π^+) and (p,π^-,π^0) Orderings

Events in the orderings (n,π^-,π^+) and (p,π^-,π^0) would populate the corner of the Dalitz plot for large $n\pi^+$ or $p\pi^0$ masses. However, both require two baryon exchanges and have a light middle particle. Their contribution is thus expected to be small, consistent with the experimental situation.

F. (π^+,π^-,n) and (π^0,π^-,p) Orderings

Although the orderings discussed in Secs. III A–III E appear to be consistent with the DRM, the orderings (π^+,π^-,n) and (π^0,π^-,p) present problems. These orderings correspond to events which would occupy the corner of the Dalitz plot for large $n\pi^+$ or $p\pi^0$ masses, as observed in Fig. 16. They are kinematically similar to the (π^-,π^+,n) and (π^-,π^0,p) orderings discussed in Sec. III A. They both involve the exchange of two meson trajectories. One expects the (π^0,π^-,p) ordering to be well populated since known meson trajectories can contribute to both exchanges, but one expects the (π^+,π^-,n) ordering to be suppressed since one of the exchanges

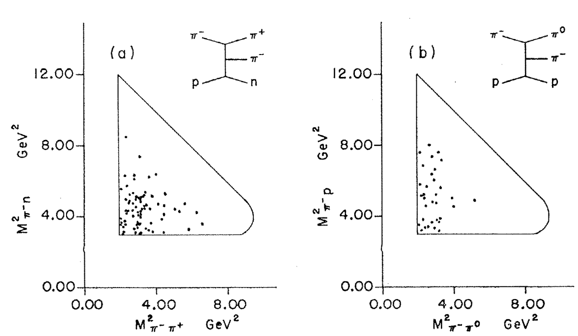

FIG. 16. Dalitz plots for events of the orderings (a) (π^+,π^-,n) and (b) (π^0,π^-,p) at 8 GeV/c.

must have $I=2$. We find that 24% (73) of the reaction (1) events and 28% (34) of the reaction (2) events in the center of the Dalitz plot are assigned to these orderings. Thus the (π^+,π^-,n) ordering compares favorably with the (π^0,π^-,p) ordering rather than being suppressed. This experimental result presents a significant difficulty for any form of DRM or double peripheral model being used to interpret the data.

Further difficulties appear when the momentum-transfer distributions for these orderings, shown in Fig. 17, are considered. Although the $|t_{25}|$ distributions appear at least as sharply peaked as the corresponding distributions in Fig. 13, the $|t_{13}|$ distributions are not. They are much broader and are quite unlike the exponential distributions expected for diffractive vertices.

We have considered several possible explanations for these discrepancies between the experimental data and DRM predictions. These possibilities include (a) the inclusion in our sample of a significant number of events involving high-mass dipion resonance production, (b) a breakdown in the event-ordering criteria, and (c) exchange of exotic resonances. These possibilities are discussed in detail in Sec. V.

G. Relations between $n\pi^+\pi^-$ and $p\pi^-\pi^0$ Final States

If definite assumptions are made about the nature of the exchange trajectories in the DRM, it is possible, in principle, to relate the contributions of a particular graph to the $n\pi^+\pi^-$ and $p\pi^-\pi^0$ channels by isospin relations. However, for these final states, several sets of exchange trajectories might contribute for each of the orderings having significant numbers of events.

For example, (P,π), (P,A), (ρ,π), and (ρ,A) exchanges could contribute to the (π^-,π^+,n) ordering while (P,π), (P,A), and (ρ,ω) exchanges could contribute to the (π^-,π^0,p) ordering. The ratio of observed events assigned to the (π^-,π^+,n) and (π^-,π^0,p) orderings is 2.35 ± 0.34. This is in reasonable agreement with the value of 2 expected for the ratio with pure (P,π) exchange in both channels. However, the agreement cannot be used to rule out the possibility of contributions from other exchanges where it is more difficult to make direct predictions. For example, the ρ trajectory can be combined with π or A exchange in the (π^-,π^+,n) case but only with ω^0 exchange in the (π^-,π^0,p) case.

In the case of the (π^-,n,π^+) and (π^-,p,π^0) orderings, where possible pairs of exchange trajectories include (P,n) and (ρ,n) in the former case and (P,p) and (ρ,p) in the latter, the expected ratio is again 2. The observed ratio is 3.8 ± 1.1. The difference might be attributed to the effects of other trajectories such as the P', to a possible breakdown in the event ordering criteria, or to the statistical fluctuations expected for small numbers of events.

In view of these uncertainties, we have not attempted to impose constraints based on isospin relations in our application of the DRM.

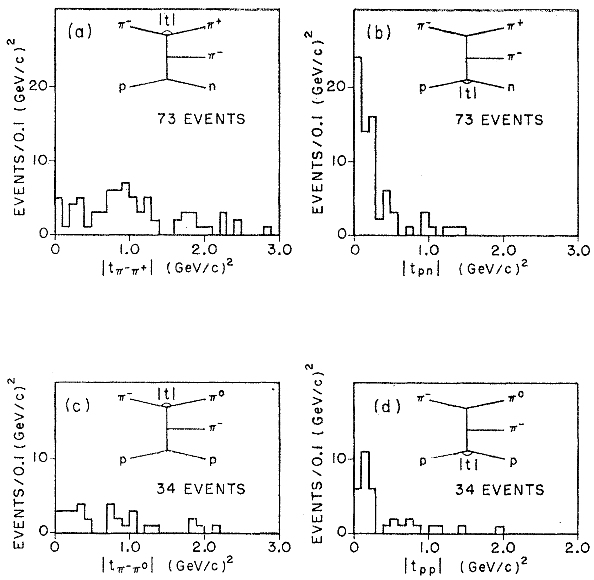

FIG. 17. Momentum transfer distributions for events of the orderings (π^+,π^-,n) and (π^0,π^-,p) at 8 GeV/c: (a) distribution of $t_{\pi^-\pi^+}$ for (π^+,π^-,n) events; (b) distribution of t_{pn} for (π^+,π^-,n) events; (c) distribution of $t_{\pi^-\pi^0}$ for (π^0,π^-,p) events; and (d) distribution of t_{pp} for (π^-,π^0,p) events.

IV. QUANTITATIVE APPLICATION OF DRM AT 8 GeV/c

As noted in Sec. III, events corresponding to the orderings (π^-,π^+,n) and (π^-,π^0,p) make up over 50% of our data and display qualitative features consistent with the DRM. Thus we have chosen this portion of our data for use in an attempt to obtain quantitative fits based on the DRM. We have been able to obtain satisfactory fits to the data and have been able to draw some conclusions about the nature of the exchanged trajectories in terms of the model.

In comparing the DRM amplitude with our data, we have assumed a graph with specific exchanges a and b (see Fig. 1). No attempt has been made to combine graphs corresponding to different exchanges either coherently or incoherently. Thus, once a specific DRM graph has been assumed, the intercepts and slopes of the linear Regge trajectories can be taken from other experimental data rather than being regarded as variables to be determined. The values used for $\alpha(0)$ and $\alpha'(0)$ for various possible exchanges are listed in Table II. In order to simplify the calculations we have assumed $\alpha'(0)=1.0$ (GeV/c)$^{-2}$ for all trajectories except the Pomeranchon trajectory for which $\alpha'(0)=0.1$ (GeV/c)$^{-2}$

TABLE II. Values used for the intercepts $\alpha(0)$ and slopes $\alpha'(0)$ of linear Regge trajectories in the DRM calculation.

Trajectory	$\alpha(0)$	$\alpha'(0)$ (GeV/c)$^{-2}$
P	1.0	0.1
π	−0.01	1.0
ρ, A, P', ω	0.5	1.0

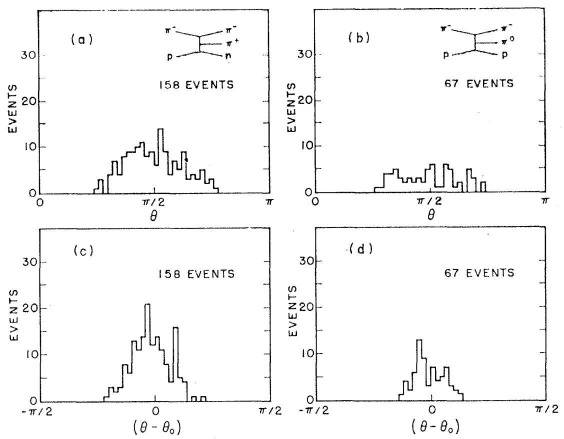

FIG. 18. Experimental distributions of the angle θ, the angle between the middle particle and the incident pion in the over-all c.m. system are shown (a) for events of the DRM ordering (π^-,π^+,n) and (b) for events of the DRM ordering (π^-,π^0,p). Also shown are distributions of $(\theta-\theta_0)$ where θ_0 is the most probable value of θ as predicted by the DRM for (c) (π^-,π^+,n) events and (d) (π^-,π^0,p) events. To obtain distributions (c) and (d), ρ- and A- or ω-meson exchanges were assumed.

has been assumed. In the remainder of the section a reference to a particular trajectory indicates the assumption of definite values for the slope and intercept.

To determine the diffractive parameters D_a and D_b [see Eq. (10)], we have used a method suggested by Chan *et al.*[2] For given values of the trajectory parameters the diffractive parameters D_a and D_b can be determined by doing a maximum-likelihood fit to the distribution of θ, the angle between particle 4 and the incoming particle 1 in the over-all c.m. system of the interaction. Once D_a and D_b have been determined, the DRM amplitude can be used to predict distributions in s_{34}, s_{45}, t_{13}, t_{25}, and the Toller angle ω. The agreement between these distributions and the corresponding experimental distributions is used as a measure of the success of the DRM with specific exchanges.

A. Determination of Diffractive Parameters

For events described by a given DRM graph, the distribution in θ is expected to have a maximum near 90°. The experimental distributions in θ for the events of orderings (π^-,π^+,n) and (π^-,π^0,p) are shown in Figs. 18(a) and 18(b). Chan *et al.*[2] have shown that, for a given set of exchange trajectory parameters, θ has a most probable value, θ_0, which may be calculated for each event in terms of the diffractive parameters D_a and D_b, and the position of the event on the Dalitz plot. For events in the center of the Dalitz plot, they have shown that the distribution $(\theta-\theta_0)$ should be peaked at 0° and be approximately Gaussian in shape. The details of the calculations and of the assumptions[17] which must be made are given in the papers cited in Ref. 2. We have used a maximum-likelihood fitting procedure to determine the values of D_a and D_b which give the best fits

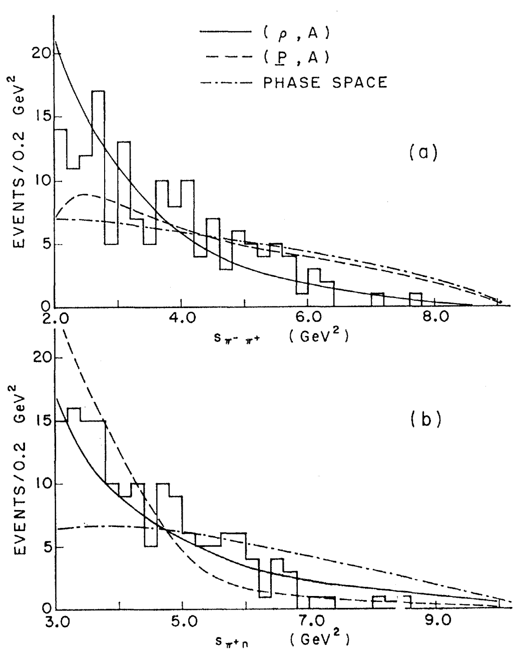

FIG. 19. Distributions of (a) $s_{\pi^-\pi^+}$ and (b) s_{π^+n} for events of the ordering (π^-,π^+,n). In addition to the experimental distributions, theoretical distributions are shown for (ρ,A) and (P,A) exchanges, and for phase space.

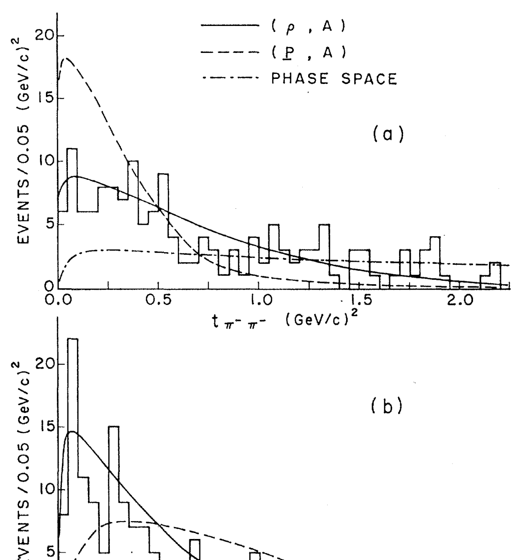

FIG. 20. Distributions of (a) $t_{\pi^-\pi^-}$ and (b) t_{pn} for events of the ordering (π^-,π^+,n). In addition to the experimental distributions, theoretical distributions are shown for (ρ,A) and (P,A) exchanges, and for phase space.

[17] We note that for this method of determining the diffractive parameters the results are independent of the intercepts of the exchange trajectories.

TABLE III. Summary of fits to diffractive parameters.

Ordering	Regge parameters assumed				Fitted diffractive parameters	
	Trajectory a	$\alpha_a'(0)$	Trajectory b	$\alpha_b'(0)$	D_a (GeV/c)$^{-2}$	D_b (GeV/c)$^{-2}$
(π^-,π^+,n)	P	0.1	π, A	1.0	2.01 ± 0.10	0.0[a]
(π^-,π^+,n)	ρ	1.0	π, A	1.0	0.14 ± 0.04	0.42 ± 0.05
(π^-,π^0,p)	P	0.1	π, A	1.0	1.92 ± 0.03	0.0[a]
(π^-,π^0,p)	ρ	1.0	ω	1.0	0.77 ± 0.09	0.99 ± 0.10

[a] In fits involving Pomeranchon exchange, D_b was constrained to be 0.0 as described in the text.

to the predicted distribution function for $(\theta-\theta_0)$.[18] In general, the fits obtained were quite reasonable. Distributions of $(\theta-\theta_0)$ are shown in Figs. 18(c) and 18(d) for the cases where the exchanged particles a and b correspond to ρ and A or ω mesons, respectively. Some difficulty was encountered in the cases where exchange a was assumed to be a Pomeranchon with $\alpha'(0)=0.1$ (GeV/c)$^{-2}$. The maximum-likelihood fits tended to yield negative values of D_b which would correspond to exponentially rising distributions for t_{25}. In these cases we constrained D_b to be 0.0 in the final fits. No such constraints were necessary in the fits involving other exchanges. Some results of fitting are listed in Table III.

B. DRM Predictions for Distributions in Kinematic Variables

Once values have been determined for the diffractive parameters for a given set of exchange trajectories, the matrix element of Eq. (10) is completely determined and can be used to calculate distributions in the subenergies s_{34} and s_{45}, the momentum transfer variables t_{13} and t_{25}, and the Toller angle ω for comparison with experimental distributions. We have generated these distributions by Monte Carlo methods.[19] Three-body $\pi\pi N$ final states in the central region of the Dalitz plot were generated. Individual events were accepted or rejected by comparing a random number to the value of the normalized DRM matrix element for the event. Once a sample of Monte Carlo events has been generated, it can be subjected to the same selections as the experimental data and distributions can be obtained in any desired variable. In Figs. 19 and 20 we show theoretical distributions in s_{34}, s_{45}, t_{13}, and t_{25}, together with the experimental distributions for events of the ordering (π^-,π^+,n). The corresponding distributions for events of the ordering (π^-,π^0,p) are shown in Figs. 21 and 22. Theoretical distributions are shown for exchanges[20] (ρ,A) or (ρ,ω) and (P,A) as well as phase-space distributions for the same cuts on the data. As expected, the phase-space distributions do not fit the data, providing further evidence that the double peripheral characteristics of the sample are not due to the selections which have been made. Distributions predicted when exchange trajectory a is the Pomeranchon trajectory of slope $\alpha'(0)=0.1$ (GeV/c)$^{-2}$ also fail to describe the data. This conclusion is not strongly dependent on the diffractive parameters used; rather it is due to the different slope of the Pomeranchon trajectory, $\alpha'(0)=0.1$. In contrast, satisfactory agreement between DRM predictions and experiment can be obtained for the exchange of trajectories if both $\alpha_a'(0)$ and $\alpha_b'(0)$ are approximately 1.0. We find that the predictions of the DRM in this case are not very sensitive to changes in

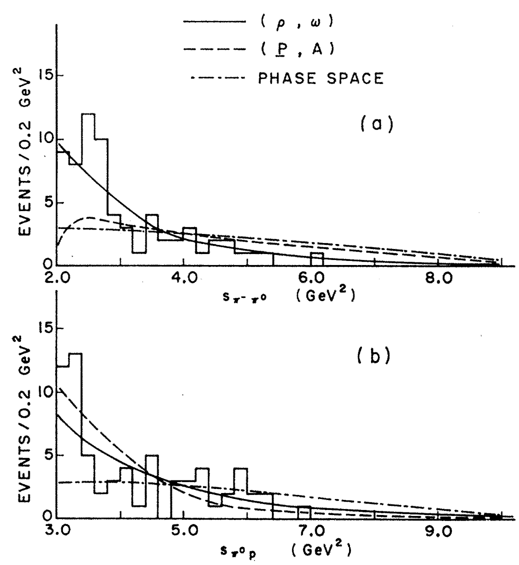

FIG. 21. Distributions of (a) $s_{\pi^-\pi^0}$ and (b) s_{π^0p} for events of the ordering (π^-,π^0,p). In addition to the experimental distributions, theoretical distributions are shown for (ρ,ω) and (P,A) exchanges and for phase space.

[18] The maximum likelihood function we have used is

$$L=\prod_{i=1}^{n}\frac{\exp[(C_i^2+D_i^2)^{1/2}\cos(\theta_i-\theta_{0i})]}{D_i\sin\theta_i},$$

where $\theta_{0i}=\tan^{-1}(D_i/C_i)$. The dependence of C_i and D_i on D_a and D_b is specified in the Appendix of Ref. 2(b). A best fit was found by maximizing $\ln L$. After a maximum was found, checks were made to ensure that the conditions used by Chan *et al.* in deriving the form for the distribution were satisfied. For example, they assume $D_i\sin\theta_i\gg1$. In a typical case we found an average value of 50 for $D_i\sin\theta_i$.

[19] We have checked the Monte Carlo distributions for s_{34} and s_{45} analytically by integrating the expression for $\partial^2\sigma/\partial s_{34}\partial s_{45}$ given by Chan *et al.* (see Ref. 2) over one of the subenergies to obtain an expression for the distribution in the other subenergy. The results agree with those obtained by Monte Carlo methods.

[20] Distributions have also been calculated for (P,π) and (ρ,π) exchanges in the (π^-,π^+,n) case and for (P,π) exchanges in the (π^-,π^0,p) case. They differ only slightly from the distributions shown where the exchanged particle b is assumed to be an A meson or ω meson.

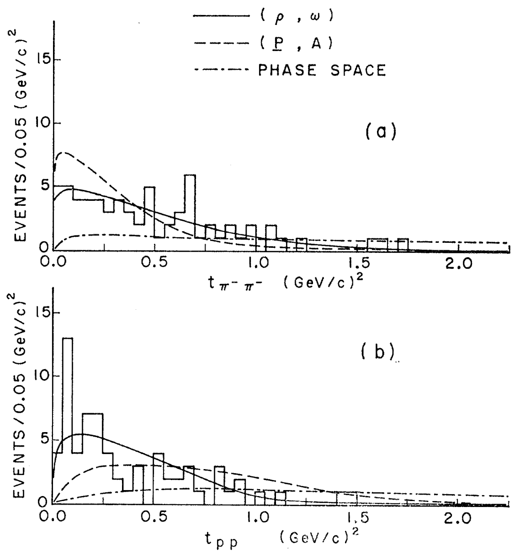

FIG. 22. Distributions of (a) $t_{\pi^-\pi^-}$ and (b) t_{pp} for events of the ordering (π^-,π^0,p). In addition to the experimental distributions, theoretical distributions are shown for (ρ,ω) and (P,A) exchanges and for phase space.

$\alpha(0)$ such as those resulting when b is taken to be a pion rather than an A meson.[20] Thus both (ρ,π) and (ρ,A) exchange pairs provide fits to the data of about the same quality. Accordingly, all the curves we show have been calculated with $\alpha(0)=1.0$ for the P trajectory and $\alpha(0)=0.5$ for the other trajectories.

In Fig. 23 are shown the experimental distributions in the Toller angle ω together with curves for phase space and for the DRM model with non-Pomeranchon exchanges. The agreement between the DRM prediction and the data is justification for our assumption that the central vertex coupling $\beta(t_{13},t_{25},\omega)$ is independent of ω. If the coupling were strongly dependent on ω we would expect this to be reflected in the failure of our DRM calculations to agree with experiment.

V. SUCCESSES AND DIFFICULTIES WITH DRM

A. Successes

We find that many features of the data for reactions (1) and (2) in the central region of the Dalitz plot may be understood both qualitatively and quantitatively in terms of the DRM. Most of the events under study appear to be multiperipheral in nature as evidenced by cornering in the Dalitz plot and by large magnitudes of longitudinal momenta for two of the outgoing particles as described in Sec. III.

Reasonable quantitative agreement has been obtained between the details of the largest subsamples of the data, the (π^-,π^+,n) and (π^-,π^0,p) orderings, and calculations based on a very simple version of the DRM which incorporates explicitly the Regge nature of the exchanges. From the results of the fitting procedure detailed in Sec. IV, we conclude that good fits can be obtained with this simple form of the amplitude using Regge trajectory parameters consistent with those needed to describe two-body final states.

Even on the basis of the simplified model, some definite conclusions can be drawn. Results are consistent with the assumption that the internal vertex function $\beta(t_{13},t_{25},\omega)$, which describes the coupling of the exchange trajectories, is independent of ω. Our results also indicate that, within the framework of the DRM, Pomeranchon exchange does not appear to dominate the reactions under study. The data can, however, be understood in terms of the DRM if both exchange trajectories are linearly rising with approximately unit slope.

The conclusion that exchange of a P trajectory of small slope does not dominate is of interest since, *a priori*, the Pomeranchon trajectory might be expected to dominate in the high-energy limit. Our result is somewhat analogous to the results of Lipes *et al.*[5] who found that double P exchange appears to be suppressed in the process $\pi^-\to\pi^-X^0p$ at 25 GeV/c even though there seems to be no obvious reason to forbid it. No similar test was made by Chan *et al.*[2] for the reaction $\pi^+p\to\pi^+\pi^0p$ at 8 GeV/c. One possible conclusion might

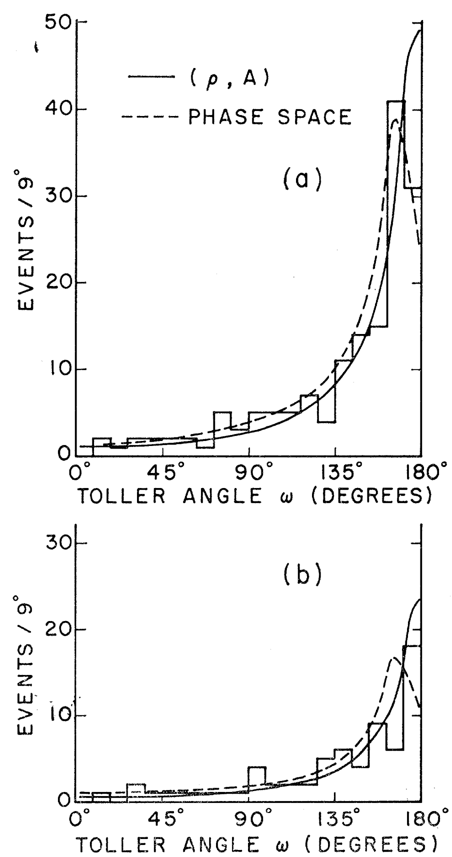

FIG. 23. Distributions of the Toller angle ω for events of the orderings (a) (π^-,π^+,n) and (b) (π^-,π^0,p). In addition to the experimental distributions, theoretical distributions are shown for (ρ,A) exchanges and for phase space.

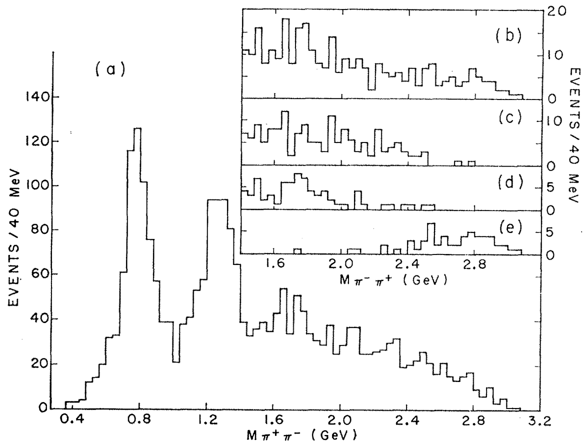

FIG. 24. Distributions of $M_{\pi^+\pi^-}$ for events of the reaction $\pi^- p \to n\pi^+\pi^-$: (a) all events; (b) events with $s_{\pi\pi} > 2$ GeV^2 and $s_{\pi n} > 3$ GeV^2; (c) events of the ordering (π^-,π^+,n); (d) events of the ordering (π^+,π^-,n); and (e) events of the ordering (π^-,n,π^+).

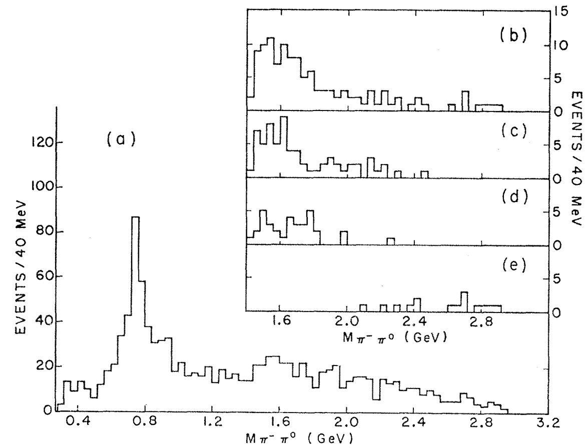

FIG. 25. Distributions of $M_{\pi^-\pi^0}$ for events of the reaction $\pi^- p \to p\pi^-\pi^0$: (a) all events; (b) events with $s_{\pi\pi} > 2$ GeV^2 and $s_{\pi p} > 3$ GeV^2; (c) events of the ordering (π^-,π^0,p); (d) events of the ordering (π^0,π^-,p); and (e) events of the ordering (p,π^-,π^0).

be that we are not yet at high enough energies for P exchange to dominate. There have also been suggestions that the Pomeranchon trajectory may not be a "typical" trajectory.[7] The slope of the Pomeranchon trajectory is not well established. Our results indicate that the assumption $\alpha_P'(0) = 0.1$ (GeV/c)$^{-2}$ is not in good agreement with the experimental distributions. Since our calculations are not very sensitive to the intercept of the trajectory,[17] it is quite possible that calculations based on a slope closer to 1.0 for the Pomeranchon or including the possibility of $P-P'$ interference would yield acceptable fits to the data.

In any case, the DRM provides a useful phenomenological model for describing three-body final states. A more detailed quantitative analysis than that discussed in Sec. IV does not seem to be warranted until a more specific version of the model can be applied to a larger sample of data at higher energies.

TABLE IV. Longitudinal momentum ordering of Monte Carlo events generated for a specific DRM diagram.

Assumed DRM ordering	Assumed exchanges	Observed ordering	Percent of events
(π^-,π^+,n)	(ρ,A)	(π^-,π^+,n)	85
		(π^+,π^-,n)	11
		(π^-,n,π^+)	4
(π^-,π^+,n)	(ρ,π)	(π^-,π^+,n)	90
		(π^+,π^-,n)	6
		(π^-,n,π^+)	4
(π^-,π^+,n)	(P,π)	(π^-,π^+,n)	78
		(π^+,π^-,n)	2
		(π^-,n,π^+)	20
(π^-,π^0,p)	(ρ,ω)	(π^-,π^0,p)	93
		(π^0,π^-,p)	5
		(π^-,p,π^0)	2
(π^-,π^0,p)	(P,π)	(π^-,π^0,p)	78
		(π^0,π^-,p)	2
		(π^-,p,π^0)	20

B. Difficulties

Despite the apparent success of the DRM in describing much of our data, there remain difficulties. In particular, an understanding of the 24% of our sample of reaction (1) included in the (π^+,π^-,n) ordering is necessary if the DRM is to be regarded as a successful model. As pointed out in Sec. III F, the events of the (π^+,π^-,n) ordering must either be described in terms of an exotic exchange or a reason for the failure of the simple DRM when applied to this subset of events must be found. Other examples exist[21] which either require the existence of exotic trajectories or present problems for exchange models. If one postulates the exchange of an $I=2$ meson trajectory, one must explain why the (π^0,π^-,p) ordering, which could be produced by exchange of either this trajectory or the ρ trajectory, is of no greater magnitude than the (π^+,π^-,n) channel. In addition, one must also explain the shapes of the $t_{\pi^-\pi^+}$ and $t_{\pi^-\pi^0}$ distributions for these events [see Figs. 17(a) and 17(c)], which do not exhibit the peaking at low $|t|$ expected from the model. At this time the evidence for the exotic mesons seems insufficient to warrant postulating their existence.

The events assigned to the (π^+,π^-,n) and (π^0,π^-,p) orderings might be qualitatively understood if our

[21] See, for example, A. Bassompierre, A. Eskreys, Y. Goldschmidt-Clermont, A. Grant, V. P. Henri, B. Jongejans, D. Linglin, F. Muller, F. M. Perreau, H. Piotrowska, J. K. Tuominiemi, G. Wolf, W. De Baere, J. Debaisieux, P. Dufour, F. Grard, P. Herquet, J. Heughebaert, L. Pape, P. Peeters, F. Verbeure, and E. De Wolf, CERN Report No. CERN/D. Ph. II/Phys. 69-20 (unpublished). They observe a peak in the four-momentum transfer squared $t_{K^+\pi^-}$ at low values, which would require exchange of a charge-2 object when interpreted in terms of a double-exchange model. They note that similar difficulties with exchange models occur in understanding the forward K^+ mesons observed in the quasi-two-body reaction $\pi^- p \to K^+ Y^{*-}$.

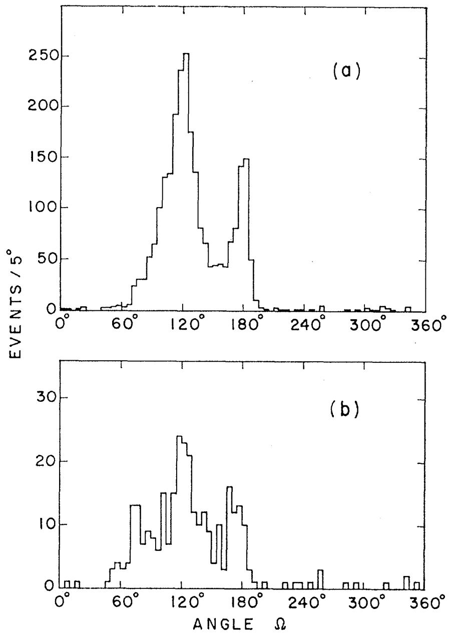

FIG. 26. Distributions of the Van Hove angle Ω with events weighted to eliminate phase-space effects: (a) all $\pi^- p \to n\pi^+\pi^-$ events and (b) $\pi^- p \to n\pi^+\pi^-$ events with $s_{\pi\pi}>2$ GeV^2 and $s_{\pi n}>3$ GeV^2.

sample of (π^+,π^-,n) data contained a considerable number of quasi-two-body events in which dipion resonances of high mass are produced. In particular, evidence for production of the g meson has been observed in our data.[16] Dipion mass distributions for events in our sample are shown in Figs. 24 and 25. Although a significant number of the events have masses in the g-meson region, no clear peaks are seen in this region or elsewhere in the dipion spectra for events in the center of the Dalitz plot or for events of the particular orderings under discussion for reaction (1). Thus there is no definite evidence for higher-mass dipion resonances in our sample. In any case no single resonance such as the g meson could account for all the events of the (π^+,π^-,n) and (π^0,π^-,p) orderings. If higher-mass boson resonances were responsible for a significant portion of our events classified as (π^+,π^-,n) and (π^0,π^-,p), the same resonances might be expected to contribute comparable numbers of events in the (π^-,π^+,n) and (π^-,π^0,p) orderings. In this case the quantitative successes of the DRM for the latter orderings would have to be regarded as at least partially fortuitous.

Another possible explanation for many of the events classified as (π^+,π^-,n) and (π^0,π^-,p) might be a failure, not of the basic DRM, but of the simple selection criteria whereby events are assigned to specific orderings. For example, Van Hove[15] has suggested that if all transverse momenta are relatively low for interactions at high c.m. energies, the DRM amplitude combined with relativistic phase space might lead to a significant fraction of events for which the ordering based on longitudinal momenta is (4,3,5) rather than the assumed (3,4,5). We have attempted to check this possibility in a number of ways.

We have examined the Monte Carlo events generated for the (π^-,π^+,n) and (π^-,π^0,p) orderings with the diffractive parameters of Table III to determine whether a significant number of such events would be classified as (π^+,π^-,n) or (π^0,π^-,p) on the basis of longitudinal momentum ordering. The results are summarized in Table IV. It appears that a significant fraction of the events in the (π^+,π^-,n) ordering might indeed come from this source. Even this fraction might be an underestimate since the possibility of misordering was not taken into account in the determination of the diffractive parameters.

We have also attempted to look at the experimental DRM amplitude, as suggested by Van Hove,[15] by weighting events with a factor to eliminate the phase-space effects and examining the weighted distributions in the Van Hove polar angle Ω. Each event was weighted by the factor

$$D_R^{-1}=E_3E_4E_5\left(\frac{\gamma_3^2}{E_3}+\frac{\gamma_4^2}{E_4}+\frac{\gamma_5^2}{E_5}\right),$$

where the E_i are the energies of the final-state particles, and γ_i is $p_l(i)/q$. The resultant distributions are shown in Figs. 26 and 27 for the events of reactions (1) and (2). The distributions look somewhat similar in form to the results of a calculation by Van Hove for events of our energy in which all tracks were required to have transverse momenta of 0.3 GeV/c. However, Van Hove's calculations indicate that the peak at 180°, corre-

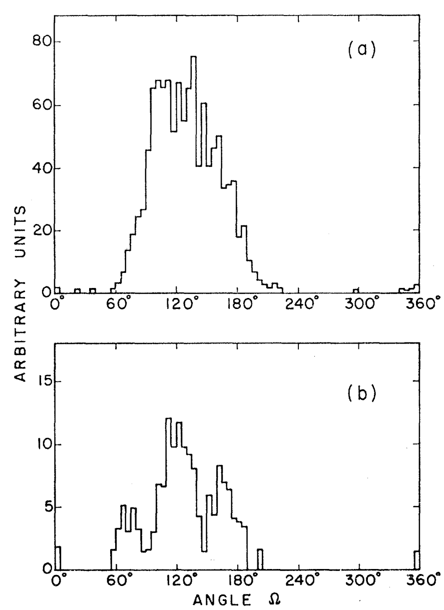

FIG. 27. Distributions of the Van Hove angle Ω with events weighted to eliminate phase-space effects: (a) all $\pi^- p \to p\pi^-\pi^0$ events and (b) $\pi^- p \to p\pi^-\pi^0$ events with $s_{\pi\pi}>2$ GeV^2 and $s_{\pi p}>3$ GeV^2.

TABLE V. Average longitudinal and transverse momentum components.

Reaction or ordering	Average longitudinal momentum (GeV/c)			Average transverse momentum (GeV/c)		
	n	π^+	π^-	n	π^+	π^-
$\pi^- p \to n\pi^+\pi^-$ (all events)	-1.415	$+0.280$	$+1.135$	0.340	0.408	0.407
$\pi^- p \to n\pi^+\pi^-$	-0.997	$+0.096$	$+0.901$	0.463	0.783	0.664
($s_{\pi\pi}>2$ GeV^2, $s_{\pi n}>3$ GeV^2)						
(π^-,π^+,n)	-1.228	0.004	$+1.225$	0.456	0.825	0.653
(π^+,π^-,n)	-1.351	$+1.142$	$+0.210$	0.486	0.785	0.628
(π^-,n,π^+)	-0.339	-1.003	$+1.343$	0.611	0.657	0.533
	p	π^-	π^0	p	π^-	π^0
$\pi^- p \to p\pi^-\pi^0$ (all events)	-1.458	$+1.124$	$+0.335$	0.381	0.389	0.367
$\pi^- p \to p\pi^-\pi^0$	-1.193	$+0.986$	$+0.207$	0.463	0.632	0.675
($s_{\pi\pi}>2$ GeV^2, $s_{\pi p}>3$ GeV^2)						
(π^-,π^0,p)	-1.355	$+1.325$	$+0.030$	0.415	0.547	0.721
(π^0,π^-,p)	-1.378	$+0.238$	$+1.140$	0.472	0.716	0.668
(π^-,p,π^0)	-0.295	$+1.329$	-1.033	0.554	0.584	0.469

sponding to a misordering of events generated for the (π^-,π^+,n) ordering, should decrease with increasing transverse momenta and be negligible by the time the transverse momenta approach 0.5 GeV/c. As shown in Table V, the average transverse momenta for events of our sample are generally on the order of 0.5 GeV/c or larger.[22] Thus we are unable to conclude definitely that Van Hove's explanation of the misordering accounts for the effect observed.

It seems quite possible that a combination of the effects considered could account for the difficulties of the simple form of the DRM. Thus the DRM seems to show promise for providing quantitative descriptions of three-body final states.[23] This can be definitely confirmed only when a more specific form of the model can be applied to a large sample of data at higher s to clarify the discrepancies observed in the application of very simple forms of the model.

If sufficient data at high s are available, a number of extensions of the present analysis would be of interest. In a more detailed form of the model more information about the exchanged trajectories, including, for example, the complete forms of the signature factors, should be included explicitly in the calculations. If data are available at several incident energies, the energy dependence of the trajectories should be included. An attempt can then be made to verify that the coupling at the vertices is independent of energy as assumed in the DRM. Other methods of determining the fitted parameters of the model, such as direct fits to the density of points on the Dalitz plots, should be investigated. If a method can be found to increase the sensitivity of the fit to the intercepts of the exchanged trajectories, further conclusions might be possible about the contributions of Pomeranchon exchange to the reactions under study. A better method of separating events of different DRM orderings is needed for study of problems such as the anomalously large fraction of events assigned to the (π^+,π^-,n) ordering. It should also be possible to include absolute normalizations for trajectories such as the pion trajectory. The model might then be used to calculate absolute cross sections for assumed exchange pairs. This would provide information about the dominance of specific exchanges in addition to checking the general validity of the model.

ACKNOWLEDGMENTS

We wish to thank the staff of the Shutt bubble chamber group and the AGS at Brookhaven National Laboratory for their assistance in this experiment. The cooperation of Professor W. Selove and the bubble chamber group of the University of Pennsylvania in allowing us access to their portion of the data is gratefully acknowledged. We also thank J. B. Annable for assistance in the data analysis, and the Notre Dame scanning and measuring staff for their efforts. The cooperation of the Notre Dame Computing Center is appreciated. Discussions with Dr. P. C. De Celles and Dr. F. Selleri during the early stages of this study were very helpful. One of the authors (W.D.S.) wishes to thank Dr. J. Mansfield for his help in understanding some of the theoretical aspects of the model.

[22] Note that the average longitudinal momentum of the π^- in events of the (π^+,π^-,n) and (π^0,π^-,p) orderings is not zero. This is another way in which these events differ from the simple DRM picture.

[23] It is of interest to point out that the DRM is consistent with a picture involving single-pion exchange together with $\pi\pi$ scattering. If this simple picture were correct, one might expect an approximation to real $\pi\pi$ scattering at one vertex and a nucleon produced at the other vertex with low-momentum transfer [see N. N. Biswas, N. M. Cason, I. Derado, V. P. Kenney, J. A. Poirier, and W. D. Shephard, Phys. Rev. Letters **18**, 273 (1967)]. Since we are studying the region of high $s_{\pi\pi}$, a forward diffraction peak should dominate, giving events corresponding to the (π^-,π^+,n) and (π^-,π^0,p) orderings; nondiffractive $\pi\pi$ scattering would contribute, in addition, to the (π^+,π^-,n) and (π^0,π^-,p) orderings but would not necessarily lead to highly diffractive t_{13} distributions.